Letter

Rigidification Dramatically Improves Inhibitor Selectivity for RAF Kinases

Amir Assadieskandar, Caiqun Yu, Pierre Maisonneuve, Igor Kurinov, Frank Sicheri, and Chao Zhang

Just Accepted

Rigidification Dramatically Improves Inhibitor Selectivity for RAF Kinases

Amir Assadieskandar,[†,#] Caiqun Yu,[†,#] Pierre Maisonneuve,[§,#] Igor Kurinov,[⊥] Frank Sicheri,[§,‖] and Chao Zhang*,[†,‡]

[†]Loker Hydrocarbon Research Institute & Department of Chemistry, University of Southern California, Los Angeles, CA 90089, USA

[‡]USC Norris Comprehensive Cancer Center, University of Southern California, Los Angeles, CA 90089, USA

[§]Lunenfeld-Tanenbaum Research Institute, Sinai Health System, Toronto, Ontario, Canada, M5G 1X5

[‖]Departments of Molecular Genetics and Biochemistry, University of Toronto, Toronto, Ontario, Canada

[⊥]Department of Chemistry and Chemical Biology, Cornell University, NE-CAT, Argonne, IL 60439, USA

KEYWORDS: rigidification, selectivity, kinase inhibitors, BRAF

ABSTRACT: One effective means to achieve inhibitor specificity for RAF kinases, an important family of cancer drug targets, has been to target the monomeric inactive state conformation of the kinase domain, which, unlike most other kinases, can accommodate sulfonamide-containing drugs such as vemurafenib and dabrafenib because of the presence of a unique pocket specific to inactive RAF kinases. We previously reported an alternate strategy whereby rigidification of a nonselective pyrazolo[3,4-d]pyrimidine-based inhibitor through ring closure afforded moderate but appreciable increases in selectivity for RAF kinases. Here, we show that a further application of the rigidification strategy to a different pyrazolopyrimidine-based scaffold dramatically improved selectivity for RAF kinases. Crystal structure analysis confirmed our inhibitor design hypothesis revealing that **21** engages an active-like state conformation of BRAF normally associated with poorly discriminating inhibitors. When screened against a panel of distinct cancer cell lines, the optimized inhibitor **21** primarily inhibited the proliferation of the expected BRAFV600E-harboring cell lines consistent with its kinome selectivity profile. These results suggest that rigidification could be a general and powerful strategy for enhancing inhibitor selectivity against protein kinases, which may open up therapeutic opportunities not afforded by other approaches.

The RAF family kinases, consisting of ARAF, BRAF and CRAF, are essential players in the RAS-RAF-MEK-ERK signaling pathway (also known as the mitogen-activated protein kinase pathway). They perform a central role in the regulation of cell proliferation, differentiation, and survival.[1] The RAF family kinases are activated by the heterotypic or homotypic dimerization of their kinase domains. The dysregulation of the dimerization and activation of RAF kinases is a potent driver of cancer and other diseases in human.[2] The most common oncogenic mutation V600E, present in 8% of all human cancers,[3] constitutively activates BRAF to drive the proliferation of a variety of cancers including melanoma, colorectal cancer and thyroid cancer.[4] In particular, nearly half of human melanomas are driven by the BRAF[V600E] mutant.[5]

Small-molecule RAF inhibitors have long been pursued as potential anti-cancer drugs. For example, sorafenib was initially developed as a RAF inhibitor over two decades ago (**Figure 1**)[6,7] was later shown to inhibit a variety of receptor tyrosine kinases in addition to RAF kinases.[8] This multi-targeted characteristic of sorafenib is thought to underlie its clinical efficacy against kidney and liver cancers but its lack of specificity (and other liabilities) has limited its broad utility against other cancers such as melanomas.[9] RAF inhibitors developed more recently, namely the sulfonamides vemurafenib and dabrafenib, display greatly improved specificity and efficacy against BRAF[V600E]-

driven melanomas leading to their approval by FDA for use in the clinic (**Figure 1**).[10]
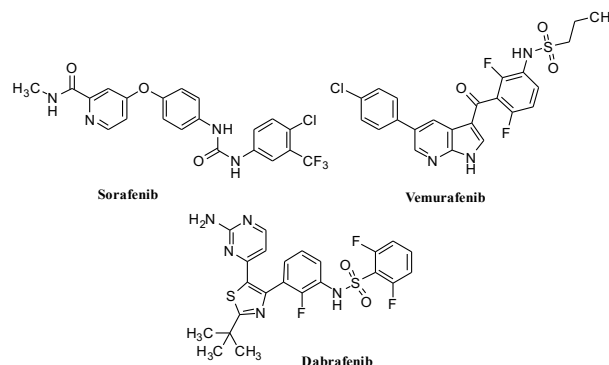
Figure 1. Chemical structures of exemplary RAF inhibitors.

In contrast to sorafenib, which targets the dimeric active state of BRAF that is generally similar to other protein kinases, vemurafenib and dabrafenib exhibits higher selectivity by targeting the monomeric inactive conformation of RAF defined by a laterally displaced helix αC.[11,12] This exploited feature is not a generally shared characteristic of kinases in their inactive states.[13,14] Despite their great initial efficacy, resistance to vemurafenib and dabrafenib develops rapidly in melanoma

patients. Because sulfonamide inhibitors share a highly related binding mode, resistance to one inhibitor would be predicted to engender resistance to all related sulfonamide chemotypes. Thus having inhibitors of RAF that are selective and yet target alternate conformations of the kinase domain would have value because they might overcome certain vemurafenib-resistant mutations.

We recently developed a rigidification strategy to improve inhibitor selectivity for the protein kinase BRAF. The first implementation of this strategy to a class of pyrazolopyrimidine-based (non-sulfonamide) kinase inhibitors led to a moderate increase of selectivity.[15] Herein, we report that a further implementation of the strategy to non-sulfonamide pyrazolo[3,4-d]pyrimidine-based inhibitors afforded a dramatic increase in selectivity for RAF kinases. Structural analysis of an optimized inhibitor confirmed our design hypothesis by revealing a binding mode that engages a dimer active-like conformation of the BRAF kinase domain. Interestingly, the optimized molecule inhibited the proliferation of cancer cells driven by BRAF[V600E] but also the proliferation of a cancer cell line NRAS[Q61R], that is normally insensitive to sulfonamides.

We previously developed 3-alkynyl-pyrazolo[3,4-d]pyrimidines, exemplified as compound **1** (**Figure 2**), as inhibitors of Bcr-Abl.[16] Although shown to be a potent inhibitor of Bcr-Abl, compound **1** inhibited many additional kinases at similar concentrations. Since our previous docking studies predicted that the benzamide groups in compound **1** was largely situated in one plane,[16] we hypothesized that changing this group into an isoquinoline ring (**Figure 2**) would introduce rigidity into the inhibitor, resulting in preferential inhibition of conformationally more flexible kinases within the kinome.[15]
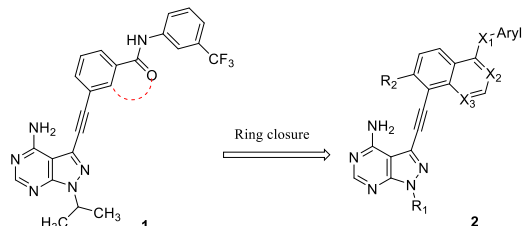

Figure 2. Cyclization of the amidobenzene group in a previously described Bcr-Abl inhibitor **1** yields compounds **2**.

To further improve kinase selectivity, a new series of alkyne-linked naphtyl, isoquinoline, or quinazoline pyrazolopyrimidines were designed (**Figure 2**) and synthesized (**Scheme 1**). The precursor compounds **3a-d** were either commercially available or synthesized based on previous literature methods. **3a** was synthesized via *N*-oxidation of 5-bromoisoquinoline with *m*CPBA followed by chlorination with phosphorus oxychloride.[17] **3c** was prepared by cyclization of 2-amino-3-bromobenzoic acid in formamide followed by chlorination with phosphorus oxychloride.[18] A precursor of **3d**, 5-iodo-6-methylisoquinoline, was made by a sequence of transformations including nitration, reduction and diazotization-iodination of 6-methylisoquinoline,[19] and then converted into **3d** using similar methods to those used for preparing **3a** (**Scheme S1**).

The intermediates **4**, except **4f**, were synthesized from compounds **3** using nucleophilic aromatic substitution reactions. **3a** and **3d**, the isoquinoline-containing precursors, were reacted with different anilines in *n*-butanol under reflux condition to

yield intermediates **4a-e** and **4i-j**.[20] Compound **4f** was made by coupling 3-(trifluoromethyl)phenylboronic acid with 5-bromo-naphthalen-1-amine in the presence of cupric acetate and triethylamine in DCM.[21] To prepare the quinazoline-containing intermediate **4g**, a milder condition involving isopropanol as solvent at room temperature was used.[18] The oxygen-linked intermediate **4h** was synthesized by refluxing 3-(trifluoromethyl)phenol, 5-bromo-1-chloroisoquinoline and K_2CO_3 in acetonitrile.[22]

The precursors **5a-c** were prepared using reported procedures with slight modifications.[23] 3-Iodo-1H-pyrazolo[3,4-d]pyrimidin-4-amine was first treated with alkyl halides to install alkyl groups at the 1 position (**Scheme S2**). The resulting intermediates underwent Sonogashira coupling reactions with trimethylsilyl acetylene and then deprotection to produce **5a-c**. In the final step, coupling of the alkyne intermediates **5a-c** with the aryl halides **4a-j** afforded the final compounds **2a-l** (**Scheme 1**).[15]
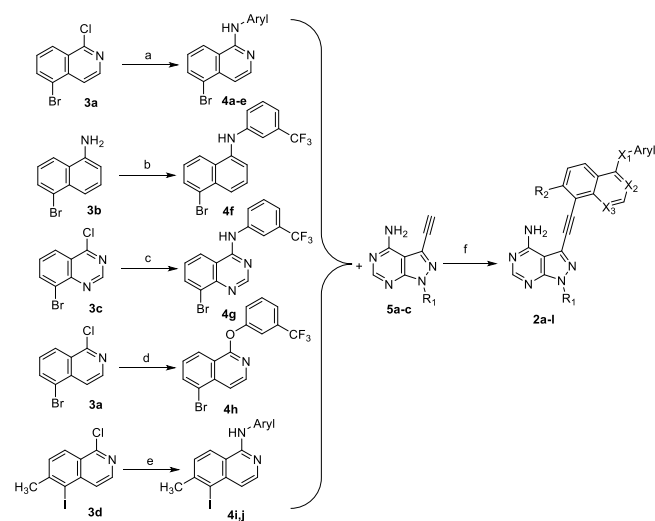
Scheme 1. Reagents and conditions: (a) aniline (3-(trifluoromethyl)aniline for **4a**, 4-chloroaniline for **4b**, 4-chloro-3-(trifluoromethyl)aniline for **4c**, 3-(4-methyl-1*H*-imidazol-1-yl)-5-(trifluoromethyl)aniline for **4d**, 4-methyl-3-(trifluoromethyl)aniline for **4e**), *n*-butanol, reflux; (b) 3-(trifluoromethyl)phenylboronic acid, Cu(OAc)₂, TEA, DCM; (c) 3-(trifluoromethyl)aniline, isopropanol, r.t.; (d) 3-(trifluoromethyl)phenol, K_2CO_3, CH₃CN, reflux; (e) aniline (3-(trifluoromethyl)aniline for **4h** and 4-chloro-aniline for **4j**), *n*-butanol, reflux; (f) (PPh₃)₂PdCl₂, CuI, DIPEA, DMF, 80 °C, N₂ (for **4a-g**); (PPh₃)₄Pd, CuI, TEA, DMF, r.t., N₂ (for **4i,j**).

We chose **2a** as a representative of the panel of synthesized compounds (**Table 1**) because of its closest structural similarity to the parent compound **1**, and evaluated its kinome inhibition profile against 245 protein kinases in comparison with **1** (**Table S1**). Consistent with our previous reported profiling results against a smaller panel of kinases,[24] the selectivity of **1** was rather poor, inhibiting 42 kinases in the panel by over 85% activity at 1 μM. In contrast, compound **2a** showed drastically improved selectivity, inhibiting only BRAF and CRAF, by over 85% activity (**Figure 3**). Hence a rigidification strategy implemented via ring closure here greatly improved the specificity characteristics of the promiscuous inhibitor **1**.
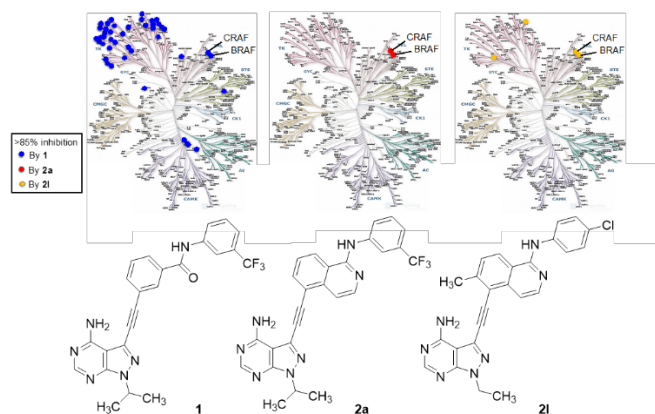
Figure 3. Kinome inhibition profiles of compounds **1** and **2a** illustrated in a phylogenetic tree format. The inhibitors were screened against 245 kinases at 1 µM. The kinases that were >85% inhibited by **1**, **2a**, **2l** are colored blue, red, and orange, respectively, on the kinome trees.

Since the kinome profiling experiment showed that compound **2a** possessed an improved specificity profile for RAF kinases, we next sought to explore the activity characteristics of the full compound series **2a-l** against BRAF, with the goal of identifying a specific lead with greatest potency. To this end we performed dose-response analyses against BRAF^{V600E} activity *in vitro* (**Table 1**). Vemurafenib, employed as a control, displayed an IC_{50} value of 21 nM, consistent with the value reported previously.[25] Compounds **2a**, **2c**, **2i**, and **2j** inhibited BRAF^{V600E} with IC_{50} values ranging between 21 nM to 140 nM while compounds **2b**, **2d**, **2e**, **2f**, **2g**, **2h** and **2k** inhibit BRAF^{V600E} with IC_{50} values greater than 300 nM (**Figure S1**). The SAR analysis indicated that a *para*-chloro substituent on the anilino moiety (as in **2c**) confers a 4-fold increase in affinity relative to a *meta*-trifluoromethyl substituent (as in **2a**). Furthermore, a methyl group at position 6 of the isoquinoline ring confers a 7-fold increase in affinity (comparing **2a** with **2i**) while an ethyl group at position 1 of the pyrazolopyrimidine relative to an *iso*-propyl group confers a 3-fold increase in affinity to BRAF (comparing **2a** and **2j**). Gratifyingly, when the favored substituents at each position were combined, the resulting compound **2l** exhibited the highest potency in the series with an IC_{50} of 8 nM against BRAF^{V600E}. This corresponded to an 18-fold increase in affinity relative to **2a**. Notably, the potency of **2l** was over two-fold more potent than vemurafenib in the same assay.

We next profiled **2l** at 1 µM against 245 kinases as performed for **1** and **2a**, and observed a slight reduction of selectivity against RAFs with just four kinases, specifically BRAF, CRAF, BRK and FMS, inhibited by more than 85% (**Figure 3**; **Table S1**). Importantly, this result demonstrated that the specificity characteristics arising from our original rigidification strategy were largely maintained following lead optimization.

Having shown that a few rigidified inhibitors were both specific and potent at inhibiting BRAF *in vitro*, we next investigated the effect of the five most potent inhibitors (**2a**, **2c**, **2i**, **2j**, and **2l**)

on the proliferation of A375 cells harboring the BRAF^{V600E} mutant (**Table 1**).[26] Notably, **2l**, the most potent inhibitor of BRAF^{V600E} of the panel *in vitro*, also displayed the highest potency at inhibiting the proliferation of A375 cells, with an IC_{50} of 417 nM, only 3-fold worse than vemurafenib (IC_{50} = 127 nM). The diminished potency of **2l** relative to vemurafenib in cells was not unexpected considering that as an FDA-approved drug vemurafenib has been greatly optimized for permeability and bioavailability. In conclusion, the optimized compound, **2l**, was effective at suppressing the proliferation of BRAF^{V600E}-driven cells, in agreement with its potent inhibition of BRAF^{V600E} *in vitro*.

We next compared the effects of **2l** with vemurafenib on downstream signaling in A375 cells. In these cells, expression of the active mutant BRAF^{V600E} leads to constitutively elevated levels of phospho-ERK (pERK), which provides a useful marker for effects on pathway signaling. In agreement with a previous report[25], vemurafenib repressed pERK levels with an IC_{50} of 80 nM, whereas **2l** inhibited phospho-ERK levels with an IC_{50} of 420 nM (**Figure 4**). These results were consistent with the relative potency of **2l** in the A375 cell proliferation assay (**Table 1**). In sum, our data showed we could use a rigification strategy to design a highly specific inhibitor that was both potent *in vitro* and in A375 cells.
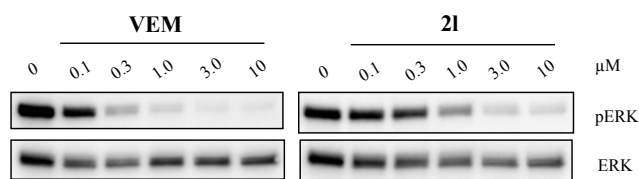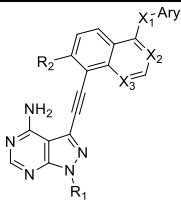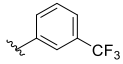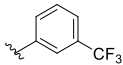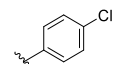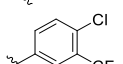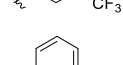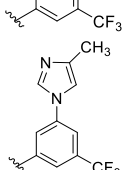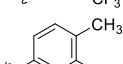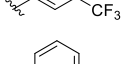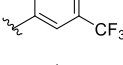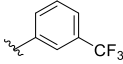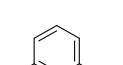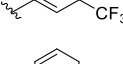

Figure 4. Effects of vemurafenib and compound **2l** on downstream signaling of BRAF^{V600E} in A375 cells. Vemurafenib and **2l** inhibited the phosphorylation of ERK with IC_{50} values of 80 nM and 420 nM, respectively.

To determine the binding mode of **2l**, we solved its co-structure in complex with the BRAF kinase domain to 3.05Å resolution (R_{work}/R_{free}= 23.5/27.5; **Table S2**). Unbiased electron density in the ATP binding pocket of each kinase domain allowed unambiguous modeling of **2l** in BRAF (**Figure 5**).

The kinase domain of RAF adopted the characteristic side-to-side dimer configuration reflective of a kinase active-like state (**Figure S2A**). This configuration, defined by a productive inward conformation of helix αC is also notably preferred by the poorly selective, non-sulfonamide inhibitor sorafenib and contrasts with the monomeric inactive-like conformation of the BRAF kinase domain engaged by sulfonamide inhibitors, which display a laterally displaced helix αC (**Figure 5B**). **2l** is stabilized in the ATP binding pocket by a mixture of hydrogen bonds and hydrophobic interactions (**Figure 5C; D**).

3

Table 1: Inhibitory activity of compounds **2a-l** against BRAF V600E and *in vitro* and in cells.

Compounds	Aryl	R_1	R_2	X_1	X_2	X_3	BRAF V600E[a] IC$_{50}$(nM)	A375[b] (BRAF^{V600E}) IC$_{50}$(nM)
2a	3-CF_3-phenyl	*i*-Pr	H	NH	N	CH	140±28	>10,000
2b	3-CF_3-phenyl	*i*-Pr	H	NH	CH	CH	>300	Nd[c]
2c	4-Cl-phenyl	*i*-Pr	H	NH	N	CH	29±10	>10,000
2d	Cl, CF_3-phenyl	*i*-Pr	H	NH	N	CH	>300	Nd[c]
2e	3-CF_3-phenyl	*i*-Pr	H	NH	N	N	>300	Nd[c]
2f	CH_3-imidazolyl, CF_3-phenyl	*i*-Pr	H	NH	N	CH	>300	Nd[c]
2g	CH_3, CF_3-phenyl	*i*-Pr	H	NH	N	CH	>300	Nd[c]
2h	3-CF_3-phenyl	*i*-Pr	H	O	N	CH	>300	Nd[c]
2i	3-CF_3-phenyl	*i*-Pr	CH_3	NH	N	CH	21±6	869±79
2j	3-CF_3-phenyl	Et	H	NH	N	CH	41±6	>10,000
2k	3-CF_3-phenyl	*n*-Pr	H	NH	N	CH	>300	Nd[c]
2l	4-Cl-phenyl	Et	CH_3	NH	N	CH	8±1	417±39
Vem							21±7	127±3

[a]IC$_{50}$ values were determined by following the *in vitro* kinase assay protocols. The data represent the mean values of two independent experiments.
[b]Growth inhibition was determined using MTT assay. A375 cells were plated in 96-well plates at 1×10^3 cells per well and incubated with different concentrations of the inhibitor for 96 h. The data represent the mean values of two independent experiments, each carried out in triplicates.
[c]Nd: not determined

Specifically, the exocyclic amino group (N^4) and the $N5$ atom of the pyrazolo[3,4-d]pyrimidine ring form hydrogen bonds with the carboxyl and the amide backbone of Gln530 and Cys532 from the hinge region, respectively. The pyrazolopyrimidine core is stabilized by hydrophobic interactions with the side chain of Phe583, Phe595, Trp531, and Ala481. The ethyl group at **1** position is poised to form hydrophobic interactions with the side chain of Ile463. The isoquinoline is stabilized by hydrophobic interactions with the Thr529, Ala481, Ile527, Lys483 and Leu514 as well as a hydrogen bond with the carboxyl backbone of Asp594 (part of the DFG loop). The aryl group of **2l** occupies the hydrophobic pocket conventionally occupied by the phenyl ring of Phe595, resulting in an outward shift of the DFG loop that is characteristic of a type-II inhibitor binding mode (**Figure 5C**). The crystal structure of the BRAF:**2l** complex also nicely explain the structure-activity relationship for the compound **2** series observed above. For example, the substitution of isoquinoline nitrogen by a carbon (as in **2b**) is unfavorable as it is expected to impair the hydrogen bond with the carboxyl backbone of Asp594 based on our crystal structure.
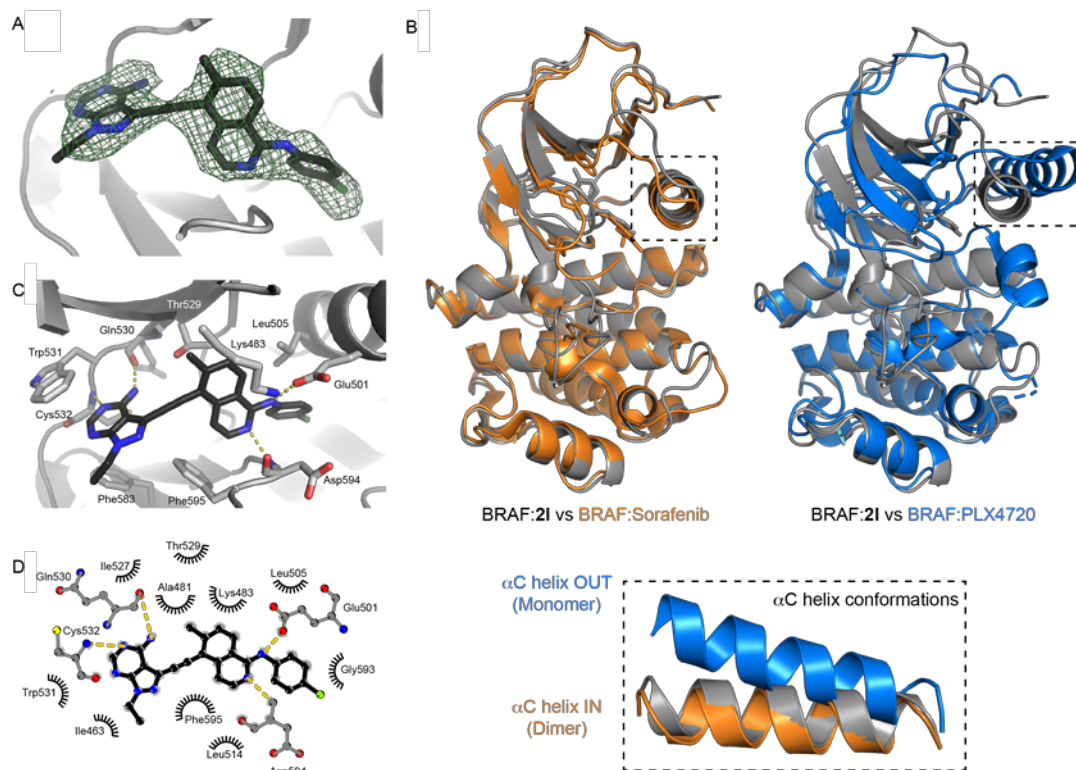

Figure 5. The X-ray crystal structures of BRAF protein in complex with **2l**. (A) Unbiased Fo−Fc electron density map contoured at 2.0σ in green showing **2l** binding in the ATP pocket of the kinase domain of BRAF. (B) Comparison of the BRAF:**2l** complex structure with (on left panel) the BRAF:sorafenib complex structure (PDB:1UWH) illustrating the dimeric ON-state conformation of the RAF kinase and with (right panel) the BRAF:PLX4720 complex structure (PDB:4WO5) illustrating the monomeric OFF-state conformation of the RAF kinase. Lower panel represents a close-up view of the inward and outward conformations of the αC helix. (C) Stick representation of **2l** bound to BRAF kinase domain. BRAF residues interacting with **2l** are represented in stick. Yellow dash lines represent hydrogen bonds. (D) Flat schematic representation of the binding mode of **2l** with BRAF. Black sticks represent hydrophobic interaction and yellow dash lines represent hydrogen bonds.

The binding mode of **2l** revealed by our structure analysis implied that, similar to other inhibitors that preferentially bind to the dimer state of RAF, that it might also promote kinase domain dimerization. To test this hypothesis further, we performed analytical ultracentrifugation analyses with recombinant BRAF kinase in the presence or absence of **2a** (**Figure S2B**). We observed that at the concentration tested, recombinant BRAF kinase sedimented predominantly as a monomer in absence of inhibitor while in the presence of saturating concentration of **2a**, BRAF sedimented mostly as a dimer. These results showed that **2a** promotes BRAF kinase dimerization. As suggested by our crystal structure showing **2l** bound to the dimer state of BRAF and based on the similar structure of compounds **2a** and **2l**, we predict that **2l** also promotes BRAF kinase domain dimerization.

To further evaluate the potency and selectivity of **2l** at inhibiting BRAF, it was screened against a collection of 57 distinct cancer cell lines at the National Cancer Institute according to the reported protocol (http://dtp.nci.nih.gov) (**Table S3**). Importantly, among the 57 cell lines, 10 harbor the BRAF[V600E] mutation. The profiling data showed that **2l** at 10 μM inhibited the proliferation of the diverse cell lines to various degrees. Notably 3 out of the 5 most sensitive cell lines (MALME-3M, MDA-MB-435 and SK-MEL-5) corresponded to melanoma cells harboring the BRAF[V600E] mutation (**Figure 6**). Further studies confirmed that **2l** inhibited the proliferation of these three cell lines in a dose-dependent manner with Total Growth Inhibition (TGI)

5

values of 7.1, 4.6, and 6.6 μM respectively. Interestingly, one of the most sensitive cell lines in the panel, SK-MEL-2, is known to harbor a mutant NRAS (Q61R). As it has been established that elevated RAS activity drive RAF dimerization in cells, these data indicate that **2l** might inhibit RAF dimers under certain cellular settings.
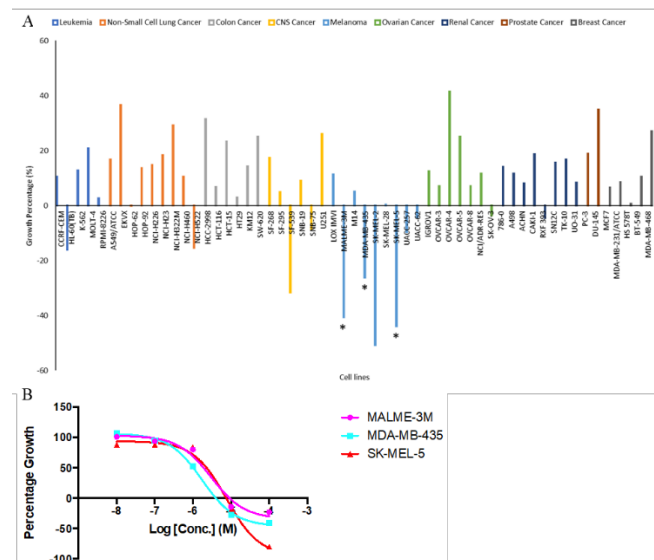
Figure 6. Compound **2l** was profiled for antiproliferative effects against diverse cancer cell lines. (A) **2l** at 10 μM preferentially inhibited the proliferation of a few out of a collection of 57 distinct cell lines. (B) **2l** inhibited dose-dependent growth inhibition of MALME-3M, MDA-MB-435, and SK-MEL-5 cells. * indicates sensitive cell lines bearing BRAF^{V600E}.

In summary, we have demonstrated that using a strategy of inhibitor rigidification, via ring closure, can lead to a dramatic increase in selectivity towards RAF kinases. Our structural and biochemical characterizations confirm that the rigidified inhibitors interact with BRAF kinase domains with a type-II binding mode that can drive RAF dimerization *in vitro*. The selectivity of our inhibitors reported here for RAF kinases is unprecedented for non-sulfonamide RAF inhibitors. We posit that, a rigidification strategy could be readily applied to other RAF inhibitor scaffolds as a potential means to generate second-generation targeted therapies where first-generation inhibitors fail to function. Furthermore, rigidification could be a general strategy for enhancing inhibitor selectivity against other protein kinases, which may open up therapeutic opportunities not afforded by other approaches.

ASSOCIATED CONTENT

Supporting Information

This material is available free of charge *via* the Internet at http://pubs.acs.org

Supplementary Figures and Tables, experimental methods, X-ray crystallography data, synthetic procedures, and compound characterization data

Accession codes. Protein Data Bank code for BRAF-**2l** complex structure is 6NSQ.

AUTHOR INFORMATION

Corresponding Author

* E-mail: zhang.chao@usc.edu

Author Contributions

The manuscript was written through contributions of all authors. All authors have given approval to the final version of the manuscript.

# These authors contributed equally to this work as first authors.

Notes
The authors declare no competing financial interest.

ABBREVIATIONS

RAF, rapidly accelerated fibrosarcoma; RAS, rat sarcoma; MEK, mitogen activated protein kinase; ERK, extracellular signal-regulated kinase; TGI, total growth inhibition.

REFERENCES

1.	Daum, G.; Eisenmann-Tappe, I.; Fries, H. W.; Troppmair, J.; Rapp, U. R. The ins and outs of Raf kinases. *Trends Biochem Sci* **1994,** 19, 474-80.
2.	Dhillon, A. S.; Hagan, S.; Rath, O.; Kolch, W. MAP kinase signalling pathways in cancer. *Oncogene* **2007,** 26, 3279-90.
3.	Bond, C. E.; Whitehall, V. L. How the BRAF V600E Mutation Defines a Distinct Subgroup of Colorectal Cancer: Molecular and Clinical Implications. *Gastroenterology research and practice* **2018,** 2018.
4.	Davies, H.; Bignell, G. R.; Cox, C.; Stephens, P.; Edkins, S.; Clegg, S.; Teague, J.; Woffendin, H.; Garnett, M. J.; Bottomley, W.; Davis, N.; Dicks, E.; Ewing, R.; Floyd, Y.; Gray, K.; Hall, S.; Hawes, R.; Hughes, J.; Kosmidou, V.; Menzies, A.; Mould, C.; Parker, A.; Stevens, C.; Watt, S.; Hooper, S.; Wilson, R.; Jayatilake, H.; Gusterson, B. A.; Cooper, C.; Shipley, J.; Hargrave, D.; Pritchard-Jones, K.; Maitland, N.; Chenevix-Trench, G.; Riggins, G. J.; Bigner, D. D.; Palmieri, G.; Cossu, A.; Flanagan, A.; Nicholson, A.; Ho, J. W.; Leung, S. Y.; Yuen, S. T.; Weber, B. L.; Seigler, H. F.; Darrow, T. L.; Paterson, H.; Marais, R.; Marshall, C. J.; Wooster, R.; Stratton, M. R.; Futreal, P. A. Mutations of the BRAF gene in human cancer. *Nature* **2002,** 417, 949-54.
5.	Mann, M. B.; Black, M. A.; Jones, D. J.; Ward, J. M.; Yew, C. C.; Newberg, J. Y.; Dupuy, A. J.; Rust, A. G.; Bosenberg, M. W.; McMahon, M.; Print, C. G.; Copeland, N. G.; Jenkins, N. A. Transposon mutagenesis identifies genetic drivers of Braf(V600E) melanoma. *Nat Genet* **2015,** 47, 486-95.
6.	Wilhelm, S.; Carter, C.; Lynch, M.; Lowinger, T.; Dumas, J.; Smith, R. A.; Schwartz, B.; Simantov, R.; Kelley, S. Discovery and development of sorafenib: a multikinase inhibitor for treating cancer. *Nature reviews Drug discovery* **2006,** 5, 835.

6

7.　　　Wan, P. T.; Garnett, M. J.; Roe, S. M.; Lee, S.; Niculescu-Duvaz, D.; Good, V. M.; Project, C. G.; Jones, C. M.; Marshall, C. J.; Springer, C. J. Mechanism of activation of the RAF-ERK signaling pathway by oncogenic mutations of B-RAF. *Cell* **2004,** 116, 855-867.

8.　　　Wilhelm, S. M.; Adnane, L.; Newell, P.; Villanueva, A.; Llovet, J. M.; Lynch, M. Preclinical overview of sorafenib, a multikinase inhibitor that targets both Raf and VEGF and PDGF receptor tyrosine kinase signaling. *Molecular cancer therapeutics* **2008,** 7, 3129-3140.

9.　　　Mousa, A. B. Sorafenib in the treatment of advanced hepatocellular carcinoma. *Saudi journal of gastroenterology: official journal of the Saudi Gastroenterology Association* **2008,** 14, 40.

10.　　　Van Allen, E. M.; Wagle, N.; Sucker, A.; Treacy, D. J.; Johannessen, C. M.; Goetz, E. M.; Place, C. S.; Taylor-Weiner, A.; Whittaker, S.; Kryukov, G. V.; Hodis, E.; Rosenberg, M.; McKenna, A.; Cibulskis, K.; Farlow, D.; Zimmer, L.; Hillen, U.; Gutzmer, R.; Goldinger, S. M.; Ugurel, S.; Gogas, H. J.; Egberts, F.; Berking, C.; Trefzer, U.; Loquai, C.; Weide, B.; Hassel, J. C.; Gabriel, S. B.; Carter, S. L.; Getz, G.; Garraway, L. A.; Schadendorf, D.; Dermatologic Cooperative Oncology Group of, G. The genetic landscape of clinical resistance to RAF inhibition in metastatic melanoma. *Cancer Discov* **2014,** 4, 94-109.

11.　　　Bollag, G.; Hirth, P.; Tsai, J.; Zhang, J.; Ibrahim, P. N.; Cho, H.; Spevak, W.; Zhang, C.; Zhang, Y.; Habets, G. Clinical efficacy of a RAF inhibitor needs broad target blockade in BRAF-mutant melanoma. *Nature* **2010,** 467, 596.

12.　　　Zhang, C.; Spevak, W.; Zhang, Y.; Burton, E. A.; Ma, Y.; Habets, G.; Zhang, J.; Lin, J.; Ewing, T.; Matusow, B. RAF inhibitors that evade paradoxical MAPK pathway activation. *Nature* **2015,** 526, 583.

13.　　　Tsai, J.; Lee, J. T.; Wang, W.; Zhang, J.; Cho, H.; Mamo, S.; Bremer, R.; Gillette, S.; Kong, J.; Haass, N. K. Discovery of a selective inhibitor of oncogenic B-Raf kinase with potent antimelanoma activity. *Proceedings of the National Academy of Sciences* **2008,** 105, 3041-3046.

14.　　　Rheault, T. R.; Stellwagen, J. C.; Adjabeng, G. M.; Hornberger, K. R.; Petrov, K. G.; Waterson, A. G.; Dickerson, S. H.; Mook Jr, R. A.; Laquerre, S. G.; King, A. J. Discovery of dabrafenib: A selective inhibitor of Raf kinases with antitumor activity against B-Raf-driven tumors. *ACS medicinal chemistry letters* **2013,** 4, 358-362.

15.　　　Assadieskandar, A.; Yu, C.; Maisonneuve, P.; Liu, X.; Chen, Y.-C.; Prakash, G. S.; Kurinov, I.; Sicheri, F.; Zhang, C. Effects of rigidity on the selectivity of protein kinase inhibitors. *European journal of medicinal chemistry* **2018,** 146, 519-528.

16.　　　Liu, X.; Kung, A.; Malinoski, B.; Prakash, G. S.; Zhang, C. Development of alkyne-containing pyrazolopyrimidines to overcome

drug resistance of Bcr-Abl Kinase. *Journal of medicinal chemistry* **2015,** 58, 9228-9237.

17.　　　Kitade, M.; Yamashita, S.; Ohkubo, S. Bicyclic compound or salt thereof. U.S. Patent 8,912,181, December 16, 2014. In.

18.　　　Kung, A.; Chen, Y.-C.; Schimpl, M.; Ni, F.; Zhu, J.; Turner, M.; Molina, H.; Overman, R.; Zhang, C. Development of specific, irreversible inhibitors for a receptor tyrosine kinase EphB3. *Journal of the American Chemical Society* **2016,** 138, 10554-10560.

19.　　　Smith, A. L.; DeMorin, F. F.; Paras, N. A.; Huang, Q.; Petkus, J. K.; Doherty, E. M.; Nixey, T.; Kim, J. L.; Whittington, D. A.; Epstein, L. F. Selective inhibitors of the mutant B-Raf pathway: discovery of a potent and orally bioavailable aminoisoquinoline. *Journal of medicinal chemistry* **2009,** 52, 6189-6192.

20.　　　Chao, Q.; Deng, L.; Shih, H.; Leoni, L. M.; Genini, D.; Carson, D. A.; Cottam, H. B. Substituted isoquinolines and quinazolines as potential antiinflammatory agents. Synthesis and biological evaluation of inhibitors of tumor necrosis factor α. *Journal of medicinal chemistry* **1999,** 42, 3860-3873.

21.　　　Chan, D. M.; Monaco, K. L.; Wang, R.-P.; Winters, M. P. New N-and O-arylations with phenylboronic acids and cupric acetate. *Tetrahedron Letters* **1998,** 39, 2933-2936.

22.　　　Gharat, L. A.; Banerjee, A.; Khairatkar-Joshi, N.; Kattige, V. G. Bicyclic compounds as mPGES-1 inhibitors. U.S. Patent 9,006,257, April 14, 2015. In.

23.　　　Zhang, C.-H.; Zheng, M.-W.; Li, Y.-P.; Lin, X.-D.; Huang, M.; Zhong, L.; Li, G.-B.; Zhang, R.-J.; Lin, W.-T.; Jiao, Y. Design, synthesis, and structure–activity relationship studies of 3-(Phenylethynyl)-1 H-pyrazolo [3, 4-d] pyrimidin-4-amine derivatives as a new class of Src inhibitors with potent activities in models of triple negative breast cancer. *Journal of medicinal chemistry* **2015,** 58, 3957-3974.

24.　　　Liu, X.; Kung, A.; Malinoski, B.; Prakash, G. K.; Zhang, C. Development of Alkyne-Containing Pyrazolopyrimidines To Overcome Drug Resistance of Bcr-Abl Kinase. *J Med Chem* **2015,** 58, 9228-37.

25.　　　Zhang, C.; Spevak, W.; Zhang, Y.; Burton, E. A.; Ma, Y.; Habets, G.; Zhang, J.; Lin, J.; Ewing, T.; Matusow, B.; Tsang, G.; Marimuthu, A.; Cho, H.; Wu, G.; Wang, W.; Fong, D.; Nguyen, H.; Shi, S.; Womack, P.; Nespi, M.; Shellooe, R.; Carias, H.; Powell, B.; Light, E.; Sanftner, L.; Walters, J.; Tsai, J.; West, B. L.; Visor, G.; Rezaei, H.; Lin, P. S.; Nolop, K.; Ibrahim, P. N.; Hirth, P.; Bollag, G. RAF inhibitors that evade paradoxical MAPK pathway activation. *Nature* **2015,** 526, 583-6.

26.　　　Poulikakos, P. I.; Zhang, C.; Bollag, G.; Shokat, K. M.; Rosen, N. RAF inhibitors transactivate RAF dimers and ERK signalling in cells with wild-type BRAF. *Nature* **2010,** 464, 427-30.

Insert Table of Contents artwork here

Rigidification Dramatically Improves Inhibitor Selectivity for RAF Kinases

Amir Assadieskandar, Caiqun Yu, Pierre Maisonneuve, Igor Kurinov, Frank Sicheri, and Chao Zhang

Non-selective kinase inhibitor   Highly selective and potent B-Raf inhibitor